Models for small-angle X-ray scattering from highly dispersed lamellae

D. J. Blundell

ICI Plastics Division, Bessemer Road, PO Box 6, Welwyn Garden City, Herts, UK

Experimental low-angle X-ray intensity profiles and their related one-dimensional correlation functions have been derived for low density polyethylene and compared with those calculated from various one-dimensional models for stacks of lamellae. Three main types of model are considered. The first type consists of 'effectively' infinite, statistically uniform stacks in which the amorphous and crystallite thicknesses follow various combinations of Gaussian and exponential distribution functions. The second type consists of statistically uniform stacks with a finite size of N lamellae. The third type introduces a dispersity between the stacks, specifically involving a variability in the local mean crystallinity. The experimental curves agree better with the last two types of model. Of these, the variable stack model is considered to be the most attractive and is interpreted in terms of phase separation during crystallization.

INTRODUCTION

Small-angle X-ray scattering from sedimented stacks of solution grown polymer crystals can give up to four orders of diffraction. This is a consequence of the low dispersity of the thicknesses of the alternating crystalline and non-crystalline 'amorphous' regions making up the stacks. In such cases, the application of Bragg's law to the first order diffraction peak is accepted as giving a good measure of the average periodic repeat distance of the structure. The diffraction profile can also be predicted reasonably with a simple one-dimensional model. In contrast to this, bulk crystallized polymers rarely give more than two orders of diffraction and many, such as low density polyethylene (LDPE), only give one broad, first order peak. In such cases it is possible that the Bragg 'long period' can be considerably distorted from the true average period of the structure[1,2]. Furthermore, it becomes more of a problem to use one-dimensional models to decide on the nature of the dispersity causing the broadening of the diffraction peak.

In this paper we are concerned with the interpretation of such broad diffraction peaks and in particular will be comparing various one-dimensional models with the diffraction patterns from LDPE. There have been several papers on the analysis of low-angle X-ray diffraction although relatively few have been specifically concerned with systems giving very broad peaks. More recently, Kilian and Wenig[3] have studied low crystallinity (40%) ethylene copolymers Ströbl and Müller[4] have given a detailed analysis of a curve from LDPE. Brown *et al.* have analysed fairly broad diffraction profiles from poly(tetramethylene oxide)[5].

In the literature there have been two main approaches to comparing experimental results with the predictions of theoretical models. The more obvious is to compare directly the intensity profiles[4,6,7]. The other is to use the device first used by Vonk and Kortleve[5,8,9] of comparing the one-dimensional correlation functions. Most authors have used one or other of the approaches, but not both at once. The two approaches tend to emphasize different aspects of the structure. Ideally, they should be equally valid if the whole of reciprocal space and real space are defined. In practice, limitations such as experimental cut-offs are unavoidable and it is possible to obtain an incomplete viewpoint by considering only one approach. For this reason we have therefore chosen to use both methods of comparison in our analyses.

In their studies, Vonk and Kortleve[8,9] derived their theoretical correlation functions by a self-convolution of their model structures and then compared these with experimental correlation functions obtained by the Fourier transformation of the corrected intensities. In the present paper both theoretical and experimental correlation functions will be derived using the Fourier transform method. While this has the advantage that any computational inaccuracies will be identical for both sets of curves, it has the slight disadvantage that the choice of fluctuation statistics in the models is restricted to those that yield analytical solutions for the intensity expressions.

Certain basic assumptions must be made when setting up a one-dimensional model for stacked lamellar systems. A good account of the nature of these is given in Ruland's recent analysis of the problem[10]. In the present paper we make the basic assumption that the lamellar stacks are effectively of infinite lateral width, so that we only have to deal with the one-dimensional variation of electron density normal to the lamellar planes. This variation will be assumed to follow a two-phase (crystal/amorphous) model where there is a sharp density transition at the crystal/amorphous interface. We will assume that the statistics of the density fluctuation along the normal of a stack can be described by Hosemann's general model[11] in which the thicknesses of the crystal and amorphous layers vary independently of each other according to prescribed distribution statistics (It should be noted that this is distinct from Hosemann's one dimension paracrystal model[2,11,12].) Using this general framework for an individual lamellar stack, three types of model will be examined.

First, will be considered the simple case where the system

0032–3861/78/111258–09$02.00

can be represented by a single stack of lamellae, where the number of lamellae is sufficiently large that the stack can effectively be considered to be of infinite height. The corresponding real sample would be composed of many such stacks which would be statistically identical so that any one stack can be taken as representative. This basic simple model has been extensively used in previous investigation[2,7,12]. Here it will be enumerated for cases where the distribution statistics describing the crystal and amorphous thicknesses are various combinations of symmetrical Gaussian distributions and asymmetric exponential distributions.

The second type of model is a more generalized form of the first and considers the case where the number of lamellae in a stack, N, is no longer large enough to be effectively infinite. Among other effects this introduces a broadening of peaks due to the finite lattice size. Kilian and Wenig[3] have recently successfully used the additional parameter, N, to match experimental curves of highly disordered copolymer systems.

In the third type of model, we will again return to 'infinite' stacks, but will now introduce a longer range inhomogeneity in which there are fluctuations between stacks as well as fluctuations of the lamellar within the stacks. The observed intensity will no longer be given by a single representative stack but will be the weighted average of the intensities of all the stacks. This is the type of model that has been proposed by Strobl and Muller[4] from their measurements of LDPE. There are many possible ways of introducing a stack dispersity of this kind. In this paper we will only consider one specific model where local crystallinity varies from stack to stack, but where the average amorphous thickness within each stack is kept constant, i.e. where the average crystalline thickness will vary in a predetermined correlated way from one stack to another. Although the details of this model are somewhat arbitrary, they were chosen to explore the possibilities of stack variability rather than as a precise postulation of the actual structure.

The experimental work of Vonk[13] has shown that the assumption made above, of a sharp interface between phases, is not upheld in practice and that transition regions of about 10 Å are often found. These finite transition regions affect the shape of the final tail of the intensity curve and the initial curvature of the correlation function. In order to eliminate this discrepancy between experimental and theoretical curves, we have made a small modification to our experimental data. The data was analysed by the methods of Ruland[14] and Vonk[13] to calculate the magnitude of the transition thickness. This value was then used to calculate the small first order correction factors needed to convert the original data into the data that would be predicted with a sharp transition. Application of these factors then enable the experimental and theoretical curves to be compared.

GENERAL FUNCTIONAL RELATIONS

In the theoretical one-dimensional models, one sets out to compute the scattered intensity $I(s)$, per unit volume of lamellar stack correctly oriented with respect to the main beam. The stacks within experimental samples will be randomly oriented with respect to the beam. Providing the lateral width of the lamellae within the stack is much larger than the 'long period' normal to the lamellae, then the one dimensional intensity $I(s)$ can be related to the observed powder type intensity profile $i(s)$ of a randomly oriented system by:

$$I(s) = 4\pi s^2 \cdot i(s) \tag{1}$$

where

$$s = \frac{2\sin\theta}{\lambda} \rightarrow \frac{2\theta}{\lambda}$$

at low angles and 2θ = angle between scattered and incident rays.

Although in principle $I(s)$ should contain all the 'information' of the lamellar periodicity, one can often get a more direct impression of the density variation in real space by following Vonk and Kortleve[8,9] and deriving the one dimensional correlation function $\gamma(r)$, using the Fourier transformation:

$$\gamma(r) = \int_0^\infty I(s)\exp\{2\pi i s r\}\,ds \tag{2}$$

The correlation function can also be defined directly in real space from the density variation along the lamellar normal by the convolution integral:

$$\gamma(r) = \int_{u=-\infty}^{\infty} \eta(u)\eta(r-u)du$$

where $\eta(u)$ is the deviation in electron density from the average density of the sample as a whole. $\gamma(r)$ is therefore a measure of the probability of finding the density to be the same for two points a distance r apart. Where there is a periodic structure, as in lamellae systems, $\gamma(r)$ can be expected to show a maximum close to values of r that are equivalent to the average repeat period. The position of this maximum can be interpreted as the most probable repeat distance rather than the precise number-average repeat distance. Typical examples are shown in *Figures 3* and *5*.

In this paper the computation of both the theoretical and experimental correlation functions is based on equation (2) and uses the same discrete fast Fourier transform analogue. This splits $I(s)$ into 256 discrete points covering the equivalent in space of about 12 orders of reflections and produces 128 discrete points for $\gamma(r)$ covering a range of r-space of about 10 periodic repeats.

Before the experimental $I(s)$ can be transformed, it is necessary to introduce two modifications similar to those used by Kortleve and Vonk[9] to account for the high and low angular regions where data is not available. The final tail was fitted to a Porod-type $1/s^2$ relationship, while the initial region up to the backstop was replaced by a function of the form s^2.

In order to aid the comparison of theory with experiment, we have chosen to characterize the main features of $I(s)$ and $\gamma(r)$ by measuring the following parameters.

From $I(s)$ curves:

L_1 = apparent Bragg long period = reciprocal of peak position

$w_{1/2}$ = ratio of (half height width of peak)/(position of peak)

From $\gamma(r)$ curves:

L_2 = position of first positive maxima

y_1 = depth of first negative peak

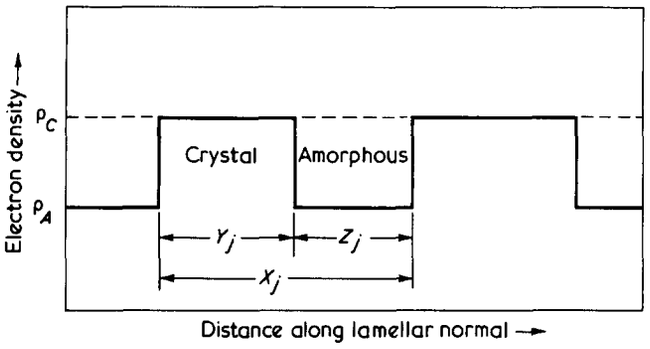

Figure 1 Basic model for lamellar stacks

y_2 = height of first positive peak

The parameters $W_{1/2}$, y_1 and y_2 are crude measurements of the curve shapes and can be used in initial comparisons as simple matching criteria.

BASIC MODEL FOR A STACK OF LAMELLAE

The variation in density through a stack along the lamellar normal will be assumed to be of the form in *Figure 1* in which the electron density varies with a rectangular profile between the crystalline value and amorphous value. The crystalline thickness, amorphous thickness and total periodic thickness of the jth lamella will be Y_j, Z_y and X_j respectively. We will use Hosemann's[11] most general model of this form in which the thicknesses Y_j and Z_j will statistically vary independently of each other and from one lamella to another. $H(Y)$ will be the normalized distribution function for the crystalline thicknesses and $h(Z)$ will be the corresponding independent distribution for the amorphous thickness. The number-average crystalline thickness will be:

$$\bar{Y} = \int H(Y) \cdot Y \mathrm{d}Y$$

and similarly:

$$\bar{Z} = \int h(Z) \cdot Z \mathrm{d}Z$$

The overall number-average long period $\bar{X} = \bar{Y} + \bar{Z}$ and the volume crystallinity of the system $\phi = \bar{Y}/\bar{X}$.

The width of the distribution functions can be characterized by the standard deviations:

$$\sigma_y^2 = \int H(Y)(Y - \bar{Y})^2 \mathrm{d}Y$$

$$\sigma_z^2 = \int h(Z)(Z - \bar{Z})^2 \mathrm{d}Z$$

Since there is no correlation between any particular Y_j and Z_j, then the standard deviation of the periodic length X_j will be:

$$\sigma_x^2 = (\sigma_y^2 + \sigma_z^2)^{1/2}$$

If a stack of N lamellae is now oriented into a diffraction position, which, in the limit of low-angle scattering, means that the lamellar normal is arranged perpendicular to the incident beam, Hosemann[11] has shown that the observable intensity profile in the plane of the normal and incident ray will be:

$$I(s) = I_B(s) + I_c(s) \tag{3}$$

$$I_B(s) = \frac{(\rho_c - \rho_A)^2}{4\pi^2 s^2 \bar{X}} \frac{|1 - F_y|^2(1 - |F_z|^2) + |1 - F_z|^2(1 - |F_y|^2)}{|1 - F_y F_z|^2} \tag{4}$$

$$I_c(s) = \frac{(\rho_c - \rho_A)^2}{2\pi^2 s^2 \bar{X} N} \mathrm{Re}\left\{ \frac{F_z(1 - F_y)^2(1 - (F_y F_z)^N)}{(1 - F_y F_z)^2} \right\}$$

where F_y and F_z are Fourier transforms of the distribution statistics e.g.

$$F_y = \int H(Y) \exp(-2\pi i s Y) \mathrm{d}Y$$

When, as in the infinite stack type of models N becomes large enough to be effectively infinite, the term I_c becomes negligible so that the observed intensity is given entirely by I_B. When N is reduced as in the finite stack type of models, I_c can no longer be neglected. It has the effect of broadening the diffraction peak and introducing a central scattering component around the main beam[11].

The expression (3) can be easily evaluated if the distribution functions $H(Y)$ and $h(Z)$ are chosen so that their Fourier transforms, F_y and F_z, reduce to simple analytical expressions. In the following sections two types of distribution function that are amenable to this analysis will be used. The first, using a Gaussian distribution, will be concerned with the properties of symmetrical distributions. The second, using a form of exponential distribution, will be used to explore the effects of asymmetry.

SINGLE INFINITE STACK MODELS

Symmetric distributions

Several past studies on one-dimensional lamellar models have shown that all symmetric distributions of corresponding width give similar results and that the Gaussian distribution is typical[9,12]. Therefore let us take $H(Y)$ and $h(Z)$ to be normalized Gaussian distributions. e.g.

$$H_1(Y) = \frac{1}{\sigma_y (2\pi)^{1/2}} \exp - \frac{(Y - \bar{Y})^2}{2\sigma_y^2}$$

where $\bar{Y}$ and σ_y are the mean and standard deviation. Similarly for $h_1(z)$. (Strictly a Gaussian will give a positive probability for negative values of Y in the negative tail. This unrealistic feature is trivial for $\sigma_y < 0.5\ \bar{Y}$ and will be ignored). The corresponding Fourier transforms have the form:

Table 1 Parameters of infinite stack model with Gaussian statistics

ϕ	σ_y	σ_2	σ_x	L_1	L_2	y_1	y_2	$W_{1/2}$
0.5	0.212	0.212	0.3	1.12	1.10	0.36	0.18	0.50
0.5	0.283	0.100	0.3	1.12	1.07	0.42	0.18	0.51
0.5	0.229	0.025	0.3	1.12	1.03	0.48	0.18	0.52
0.5	0.0707	0.0707	0.1	1.00	1.00	0.77	0.69	0.06
0.6	0.0832	0.0551	0.1	1.00	1.00	0.65	0.67	0 06
0.75	0.0947	0.0316	0.1	1.00	1.00	0.35	0.59	0.06
0.5	0.141	0.141	0.2	1.03	1.02	0.54	0 38	0.26
0.6	0.166	0.111	0.2	1.03	1.02	0.51	0.36	0.26
0.75	1.89	0.063	0.2	1.03	1.02	0.32	0.26	0.26
0.5	0.212	0.212	0.3	1.12	1.10	0.36	0.18	0.50
0.6	0.250	0.167	0 3	1.12	1.10	0.34	0.17	0.53
0.75	0.284	0.095	0.3	1.10	1.09	0.26	0.11	0.65
0.5	0.283	0.283	0.4	1.30	1.25	0.24	0.094	0.82
0.6	0.333	0.222	0.4	1.28	1.23	0.24	0.086	0.84
0.75	0.379	0.126	0.4	1.21	1.18	0.19	0.056	1.2

$$F_y = \exp(-2\pi^2 s^2 \sigma_y^2)\cdot\exp(-2\pi i s\bar{Y})$$

These can be substituted in equations (4) to give the intensity expression $I(s)$.

It is convenient to evaluate this expression by making $\bar{X} = 1.0$, so that the independent variables are then σ_y, σ_z and crystallinity ϕ. For the case of perfect regularity (i.e. $\sigma_y = \sigma_z \to 0$), one would then expect from Bragg's law that the first order diffraction peak of $I(s)$ would occur at $s = 1.0$. Similarly one would expect $\gamma(r)$ to exhibit a positive correlation peak at $r = 1.0$. As the distributions are made broader the peaks in both functions will distort and shift from these positions.

Table 1 lists how the main features of $I(s)$ and $\gamma(r)$ vary with selected combinations of σ_y, σ_z and ϕ.

The first group of samples in this *Table* show the effect of various combinations of σ_y and σ_z keeping ϕ and the overall standard deviation σ_x fixed. The second group of results show different combinations of ϕ and σ_x, such that σ_y and σ_z are related by $\sigma_y/\bar{Y} = \sigma_z/\bar{Z}$, i.e. relative deviations are identical for crystalline and amorphous thicknesses.

Not surprisingly, the main features of the curves are dependent on more than one model parameter, especially as the distributions are made broader. However the following trends are worth noting, some of which are well known.

(i) The half-width $W_{1/2}$ is mainly dependent on the overall deviation σ_x. This result is well known from the work of Hosemann[11].

(ii) For ϕ in range 0.4 to 0.6, the correlation peak heights y_1 and y_2 are insensitive to changes in ϕ. This was first demonstrated by Kortleve and Vonk[9].

(iii) If ϕ and σ_x are kept constant, then y_2 and $W_{1/2}$ are almost invariant to changes in the relative sizes of σ_y and σ_z. Providing also that σ_y and σ_2 are kept reasonably balanced, then y_1 also becomes relatively insensitive. If either σ_y or σ_z is made very small compared with the other, then y_1 increases.

(iv) As expected, L_1 and L_2 are closely related to each other. When σ_x is increased, both peaks in $I(s)$ and $\gamma(r)$ become distorted so that L_1 and L_2 move to positions greater than unity. For $\sigma_x > 0.3$, this distortion is quite significant.

Asymmetric thickness distribution

Asymmetric distributions have been explored in the past particularly to look for effects of asymmetry on the distortion of the diffraction peak. Tsvankin[6], used a simple exponential distribution:

$$H(Y) = \frac{1}{\sigma_y}\exp(-Y/\sigma_y)$$

This introduces some confusion since the number-average thickness is then identical with the standard deviation σ_y so that the effects of mean thickness cannot be separated from those due to dispersion. In the present study this is overcome by the minor modification of displacing the abscissa a distance of Y_0. Thus,

$$H_2(Y) = \frac{1}{\sigma_{y*}}\exp\left\{-\frac{(Y - Y_0)}{\sigma_{y*}}\right\} \quad \text{for } Y \geqslant Y_0$$

$$= 0 \qquad \text{for } Y < Y_0$$

In this case, the standard deviation = σ_{y*} and the number average thickness $\bar{Y} = Y_0 + \sigma_{y*}$. $H_2(Y)$ then reduces to the Tsvankin case when $Y_0 = 0$. The amorphous distribution $h_2(Z)$ is also defined by a similar expression. As before, the overall standard deviation will be defined as $\sigma_{x*} = (\sigma_{y*}^2 + \sigma_{z*}^2)^{1/2}$ and the number-average period $\bar{X} = \bar{Y} + \bar{Z}$. The Fourier transforms of these distributions have the form:

$$F_y = \frac{1}{1 + 2\pi i s\sigma_{y*}}\exp(-2\pi i s Y_0)$$

It is convenient to discuss the results obtained by substituting these expressions in equation (4) later, together with the results of the next section.

Mixed thickness distribution

A useful combination of the symmetrical and asymmetrical distributions can be obtained by using a distribution

Table 2 Parameters of infinite stack model with mixed Gaussian and exponential statistics

	Gaussian		Exponential							
ϕ	σ_y	σ_z	σ_{y*}	σ_{z*}	σ_x	L_1	L_2	y_1	y_2	$w_{1/2}$
0.5	–	–	0.141	0.141	0.2	0.97	0.95	0.61	0.42	0.22
	0.1	0.1	0.1	0.1	0.2	1.01	0.99	0.56	0.38	0.25
	0.141	0.141	–	–	0.2	1.03	1.02	0.54	0.38	0.26
0.5	–	–	0.212	0.212	0.3	0.93	0.90	0.40	0.20	0.51
	0.15	0.15	0.15	0.15	0.3	1.08	1.03	0.36	0.17	0.53
	0.212	0.212	–	–	0.3	1.12	1.10	0.36	0.18	0.50
	0.212	–	–	0.212	0.3	1.04	1.00	0.38	0.18	0.52
	0.283	–	–	0.1	0.3	1.11	1.04	0.43	0.18	0.52
	0.1	–	–	0.283	0.3	0.93	0.92	0.45	0.24	0.41
	0.299	0.025	–	–	0 3	1.12	1.03	0.48	0.18	0.52
0.5	–	–	0.283	0.283	0.4	0.93	0.85	0 20	0.06	–
	0.2	0.2	0.2	0.2	0.4	1.22	1.12	0.22	0.07	–
	0.283	0.283	–	–	0.4	1.30	1.25	0.24	0.09	0.82

Table 3 Parameters for finite stack model

ϕ	σ_x	N	L_1	L_2	y_1	y_2	$w_{1/2}$
0.5	0.2	∞	1.03	1.02	0.58	0.38	0.26
		100	1.03	1.02	0.58	0.38	0.26
		10	1.03	1.02	0.56	0.33	0.29
		5	1.05	1.04	0.52	0.27	0.34
		2	1.18	1.12	0.50	0.19	0.62
0.5	0.25	∞	1.08	1.06	0.50	0.26	0.37
		5	1.10	1.08	0.45	0.18	0.53
		2	1.23	1.16	0.43	0.11	0 68
0.5	0.3	∞	1.12	1.10	0.43	0.17	0.50
		5	1.16	1.13	0.40	0.12	0.64
		2	1.30	1.23	0.38	0.09	0.77

function H_3 which is a convolution of a Gaussian and displaced exponential form.

$$H_3(Y) = \int_{-\infty}^{\infty} H_1(p)H_2(Y-p)\,dp$$

where

$$H_1(Y) = \frac{1}{\sigma_y(2\pi)^{1/2}} \exp\left(-\frac{Y^2}{2\sigma_y^2}\right)$$

$$H_2(Y) = \frac{1}{\sigma_{y*}} \exp -\frac{(Y-Y_0)}{\sigma_{y*}}$$

$H_3(Y)$ does not have a simple analytical form. However in the general expression 3, $H_3(Y)$ is only involved as a Fourier transform. We can therefore use the well known relationship for the transform of a convolution product.

$$\mathcal{F}(H_3) = \mathcal{F}(H_1)\,\mathcal{F}(H_2)$$

where $\mathcal{F}$ is the Fourier transform operator.

This transform has the property that if either σ_y or σ_{y*} approach zero, then $\mathcal{F}(H_3)$ degenerates into the transform of either a pure exponential or a pure Gaussian distribution. The resulting expression for $I(s)$ obtained by using this form of transform thus allows one to explore all types of combination of symmetrical and asymmetrical behaviour. Examples of the main features of $I(s)$ and $\gamma(r)$ for this combined model are shown in *Table 2.*

The most obvious differences between a pure exponential and pure Gaussian seen in this Table is that the exponential case causes a decrease in L_1 and L_2 as the overall deviation σ_x is increased. This general effect of asymmetrical distributions was first noted by Rheinhold *et al.*[1]. Mixtures of exponential and Gaussian statistics in various combinations give unspectacular hybridized behaviour.

Of particular importance is that despite the behaviour of L_1 and L_2 neither of the parameters y_1, y_2 and $w_{1/2}$ vary markedly from the magnitudes seen for corresponding pure Gaussian distributions, for comparable values of σ_x and ϕ.

FINITE LAMELLAR STACK MODEL

We now consider the type of model where the number of lamellae in each stack is reduced to a level that the term $I_c(s,N)$ can no longer be neglected. Hosemann has demonstrated that this term introduces a central scatter around the main beam and also has the effect of broadening the diffraction peak given by the $I_B(s)$ term.

The presence of the central scatter poses a difficulty in our task of comparing correlation functions, since the Fourier transform of this added scatter causes the whole pattern to be raised and distorted, thus making it impossible to determine the parameters y_1 and y_2 needed for model comparison. However since much of the central scatter is in the range of s that is experimentally behind the backstop, we have modified the theoretical curves by arbitrarily imposing an artificial backstop in the region $s < 0.5$. The intensity function has then been replaced in this region with an extrapolated s^2 curve, in the same way as the experimental intensity curves. This procedure then gives well behaved correlation functions. Examples of the curve parameters obtained for this model are shown in *Table 3.* For simplicity, Gaussian statistics are used in equation (3), where $\sigma_y/\bar{Y} = \sigma_z/\bar{Z}$.

It will be noted that there is little change from the infinite stack case until N is reduced to 10 lamellae per stack, and no exceptional change occurs until N is below 5. *Table 3* clearly shows the increase in peak broadening as N is decreased. There is also a corresponding decrease in y_1 and a particularly marked decrease in y_2.

It is also of interest to compare the results for N = ∞ with the corresponding results in *Table 1*, in order to note the effect of the 'experimental' backstop at $s = 0.5$. Clearly this cut-off will not change the halfwidth of the $I(s)$ curve itself. However it does have the effect on the transform of significantly increasing y_1 but leaving y_2 relatively unaltered.

VARIABLE STACK MODEL

We now consider the situation where there is a fluctuation in the overall composition of the stacks. The net intensity can no longer be represented by a single statistical stack but will be the average of the whole stack distribution.

There are many ways in which a fluctuation between stacks can be envisaged. Here a specific model will be considered in which the overall local crystallinity varies from one stack to another. This situation could arise due to an inhomogeneity in polymer composition giving rise to fractionation effects, or due to a variation in crystallization conditions through the sample.

We will describe the variation in crystallinity in the sample by the normalized distribution function $P(\phi)$ which gives the probability of a given crystallinity occurring in a given volume of stacks. The net observed intensity per unit volume will be the volume-average of the intensities of the component single stack intensities. Thus

$$I(s) = \int I(s,\phi) \cdot P(\phi) \mathrm{d}\phi$$

The overall crystallinity $\bar{\phi}$ of the system and the dispersion σ_c of the stack crystallinity will be given by:

$$\bar{\phi} = \int \phi P(\phi) \mathrm{d}\phi$$

$$\sigma_c^2 = \int (\phi - \bar{\phi})^2 P(\phi) \mathrm{d}\phi$$

This proposed crystallinity fluctuation is insufficient to specify the model fully. It is necessary to make a further assumption concerning how the overall period in each stack is related to the local stack crystallinity. Let us therefore consider the specific case where the average amorphous thickness is constant for all lamellar stacks and independent of the local crystallinity of the stack, so that the local long period will therefore be larger in those stacks where the crystallinity is higher. If Z_0 is this common average amorphous thickness, then the local long period will be given by:

$$\bar{x}(\varphi) = Z_0/(1 - \phi)$$

It is easy to show that the overall number-average long period of the whole system is simply:

$$\bar{\bar{x}} = Z_0/(1 - \bar{\phi})$$

The assumption of a constant average amorphous thickness is not entirely arbitrary, since we have often observed the trend when samples from the same polymer family are crystallized under differenct conditions.

Results in the literature also often show this trend[9]. It has the implication that the long period is largely governed by a characteristic amorphous thickness.

This model has been evaluated for cases where $P(\phi)$ is a Gaussian distribution. In order to avoid unrealistic situations and singularities when $\phi \to 1.0$, the numerical integration was curtailed to $\phi < 0.95$. For simplicity, the intrinsic intensity for each component stack, $I(s,\phi)$, was taken to be the pure Gaussian case with:

$$\sigma_y/\bar{Y} = \sigma_z/\bar{Z}$$

Typical results are listed in *Table 4*. The introduction of stack dispersity produces a decrease in both y_1 and y_2. The most dramatic effect is the proportionally larger decrease of y_2 with respect to y_1. This trend is linked with a marked increase in halfwidth $W_{1/2}$ of the intensity function. The decrease in y_2 can be considered to be the result of taking the volume-average of the correlation functions from different stacks in which the first positive correlation peaks tend to be cancelled out by the negative troughs from other differing stacks.

EXPERIMENTAL

Two grades of LDPE from ICI were used. Polymer A had an *MFI* = 0.3 and a reference density of 0.924 kg/m^3, while Polymer B had an *MFI* = 2.0 and a reference density of 0.920 kg/m^3.

The samples prepared from these polymers are listed in *Table 5*. The slow cooled samples were made by compression moulding 1 mm thick sheets between glazing plates at 160°C and then cooling the press at a controlled rate. The quenched samples were made by pressing 0.3 mm sheets at 160°C and quenching into a CO_2/acetone mixture. The low-angle X ray scatter $J(s)$ was obtained from a slit collimated Kratky Camera and recorded with a CGR Linear Position Sensitive Detector and an Elliott Processor Unit.

Table 4 Parameters for variable stack model

ϕ	σ_x	σ_c	L_1	L_2	y_1	y_2	$w_{1/2}$
0.5	0.1	0	1.00	1.0 0	0.77	0.69	0.06
0.5	0.1	0.15	1.05	0.95	0.52	0.18	0.65
0.5	0.1	0.2	1.04	0.95	0.45	0.103	0.75
0.5	0.1	0.25	1.04	0.93	0.41	0.066	0.83
0.5	0.15	0	1.01	1.00	0.65	0.53	0.15
0.5	0.15	0.1	1.06	1.02	0.53	0.265	0.51
0.5	0.15	0.15	1.08	1.02	0.46	0.16	0.68
0.5	0.15	0.2	1.08	1.02	0.42	0.101	0.78
0.5	0.15	0.25	1.08	1.02	0.38	0 068	0.84
0.5	0.2	0	1.03	1.02	0.54	0.38	0.26
0.5	0.2	0.1	1.12	1.04	0.44	0.21	0.58
0.5	0.2	0.15	1.14	1.05	0.40	0 13	0.74
0.5	0.2	0.2	1.15	1.06	0.36	0.086	0.83
0.5	0.2	0.25	1.18	1.06	0 34	0.065	0.87
0.5	0.3	0	1.12	1.10	0.36	0.18	0.50
0.5	0.3	0.1	1.22	1.15	0.32	0.125	0.71
0.5	0.3	0.15	1.28	1.17	0.30	0.087	0.86
0.5	0.3	0.2	1.29	1.21	0 28	0.062	0.93
0.5	0.3	0.25	1.32	1.22	0.27	0.049	1.00

Table 5 Parameters from experimental curves

Sample No.	Polymer	Cooling rate	ϕ	L_1 (nm)	L_2 (nm)	y_1	y_2	$W_{1/2}$	Estimated from variable stack model σ_x	σ_c
1	A	Quench	0.45	11.3	10.7	0.46	0.14	0.69	0.175	0.15
2	A	1½°C/min	0.48	12.2	11.8	0.33	0.06	0.88	0.2	0.25
3	A	6°C/hr	0.50	13.5	12.7	0.30	0.05	0.96	0.2	>0.25
4	B	Quench	0.42	10.8	10.1	0.41	0.10	0.85	0.2	0.175
5	B	1½°C/min	0.47	12.0	11.2	0.36	0.07	0.88	0.2	0.25

A correction for the continuous background was made by subtracting a constant background deduced from the asymptote at higher angles[13]. The transition thickness E at the phase boundaries was then determined from a $J \cdot s^3$ *versus* s^2 plot using the method of Ruland[14] and Vonk[13]. The slit smeared intensities were then multiplied by a factor

$$\left(1 - \frac{2\pi^2 E^2 s^2}{3}\right)^{-1}$$

to correct them to what they would have been if the system had had sharp phase boundaries. These intensities were then desmeared and then multiplied by $4\pi s^2$ as in equation (1) in order to obtain the equivalent 'one-dimensional' scattered intensity. A smooth asymptotic curve of the form $1/s^2$ was then fitted to the tail[9] and the initial part up to the backstop replaced by a curve of the form s^2. The experimental one-dimensional correlation function was then evaluated using the same fast Fourier transform analogue as used for the theoretical cases.

The main features of the results are summarized in *Table 5*. The values for volume crystallinity in this *Table* are based on density and X-ray crystallinity measurements. It will be noticed that as the crystallization cooling rate is decreased, y_1 and particularly y_2 both decrease and the relative half-width increases, apparently indicating a decrease in long range order.

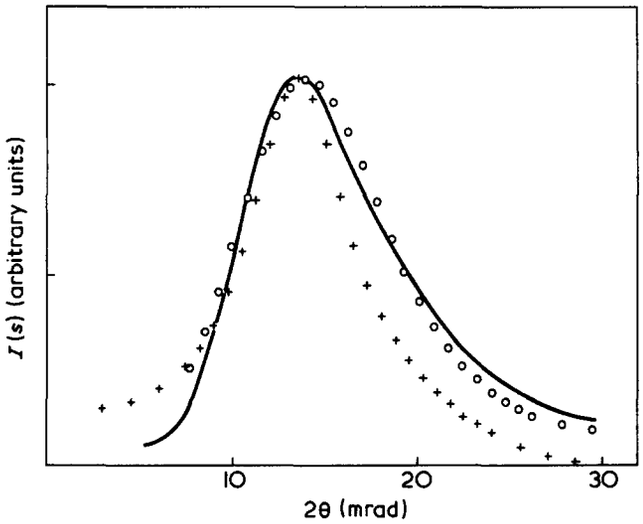

Figure 2 Experimental intensity $I(s)$ plot for sample 1, with superimposed, scaled, theoretical points for: ○, variable stack model, $\phi = 0.5$, $\sigma_x = 0.175$, $\sigma_c = 0.15$; +, infinite stack model, $\phi = 0.5$, $\sigma_y = 0.299$, $\sigma_z = 0.025$

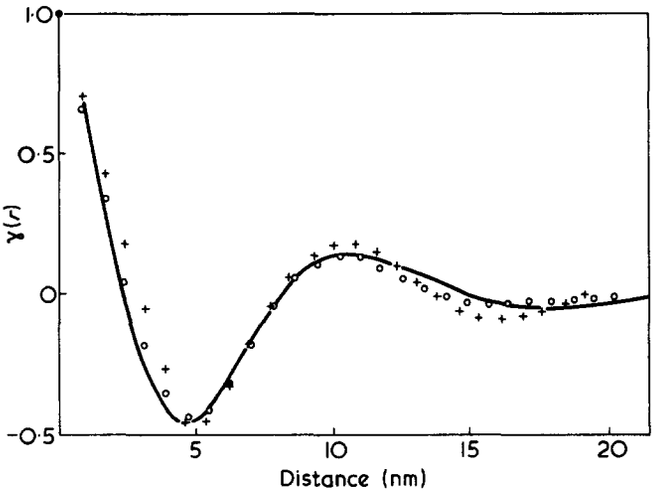

Figure 3 Correlation function for sample 1, with superimposed, scaled theoretical points for: ○, variable stack model, $\phi = 0.5$, $\sigma_x = 0.175$, $\sigma_c = 0.15$; +, infinite stack model, $\phi = 0.5$, $\sigma_y = 0.299$, $\sigma_z = 0.025$

COMPARISON WITH MODELS

All the experimental samples have a crystallinity between 0.4 and 0.6. This is the range over which the $I(s)$ and $\gamma(r)$ curves are relatively insensitive to a difference in crystallinity. Hence for the purpose of a general comparison it is valid to compare the experimental results with theoretical calculations based on $\phi = 0.5$.

For an initial sorting, it is useful to focus just on the curve parameters y_1 and y_2 and to compare the experimental results with *Tables 1* and *2* for the infinite single stack type of models. The agreement is generally poor in that for a given match in y_1, the related experimental values of y_2 are significantly lower than the y_2 of the single stack models. This conclusion holds for cases where the crystalline and amorphous thicknesses obey symmetrical Gaussian statistics, where they obey asymmetrical exponential statistics and where the statistics are mixed in all combinations of symmetric and asymmetric distributions. The closest approach to experiment in this set is when either σ_y or σ_z become vanishingly small: e.g. compare sample 1 with $\sigma_y = 0.299, \sigma_z = 0.025$ in *Table 1*. The plots of this comparison are shown in *Figures 2* and *3*. [The situation when $\sigma_z \to 0$ is also the one that Brown *et al* [5] found gave a good fit of correlation functions in their study of poly(tetramethylene oxide).] However although y_1 and y_2 may be close, the agreement with $I(s)$ curves is poor, the experimental value of $W_{1/2}$ being much higher than that of the models. A further criticism of this situation is that the theoretical $I(s)$ curve goes to almost zero intensity around $s = 2.0$. (This is a direct consequence of making $\sigma_z \to 0$ and can be regarded as a missing

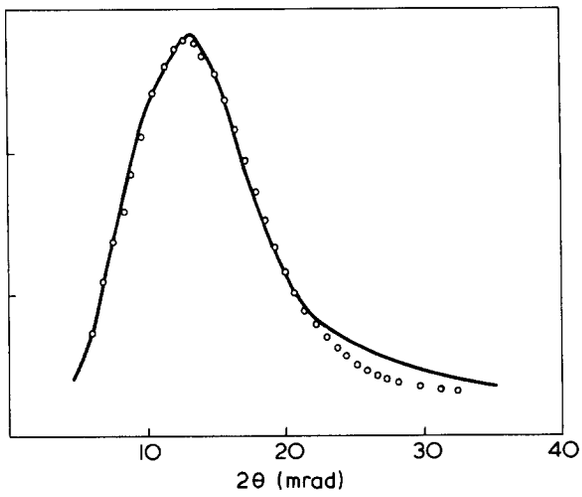

Figure 4 Experimental intensity plot for sample 5, with superimposed, scaled theoretical points for the variable stack model with $\phi = 0.5$, $\sigma_x = 0.2$, $\sigma_c = 0.25$

order effect resulting from the interaction of the 'particle factor' with the 'lattice factor'[12]). Apart from these deficiencies in the $I(s)$ curve, the physical situation with either $\sigma_y = 0$ or $\sigma_z = 0$ is unrealistic for polymer crystals in that it implies that either the crystalline or amorphous thickness is invariant.

Another situation where the infinite stack model gives a close approach to experimental values of y_1 and y_2 is in *Table 3* for the case when $N \to \infty$: e.g. compare sample 1 with $\sigma_x = 0.3$, $N = \infty$. This case is in fact identical to the entry for $x_y = \sigma_z = 0.212$ in *Table 1*, with the important exception that the initial backstop region, $s < 0.5$, has been replaced with an s^2 curve. Again however the theoretical $W_{1/2}$ is too small and there is poor agreement with the shape of the $I(s)$ curves. Both this and the previous example with $\sigma_z = 0$ illustrate the difficulties of relying only on a cursory match of $\gamma(r)$ curves, and not also checking the $I(s)$ curves.

Better success at matching all three curve parameters y_1, y_2 and $W_{1/2}$ can be obtained using either the finite stack model (*Table 3*) or the variable stack model (*Table 4*). Other details of the curves also show a better fit. Examples of comparative plots of samples 1 and 6 against scaled curves for the variable stack model are shown in *Figures 2* and *5*. Acceptable comparative plots can be obtained for both models with a suitable choice of parameters. However to do this for the finite stack model requires using values of $N \sim 2$, which is approaching the limit of the concept of a 'stack' of lamellae. Order of magnitude estimates of the parameters needed to fit the variable stack model are given in *Table 5*. These values are consistent with an increase in stack dispersion as the cooling rate is decreased.

DISCUSSION

The above comparison indicates that the simple infinite stack type of models can be eliminated as appropriate models for LDPE. Although still imperfect, better fits can be obtained with either the finite stack or variable stack models. Purely as an exercise in curve fitting there is little to choose between them, although the variable stack model is marginally better. It is not possible from diffraction data alone, to conclude that either of these models are representative of the real structure. However the two models can still be used to show the type of structural modification needed to simulate the observed diffraction behaviour and it is therefore worth considering further some of their implications.

In order to approach the observed behaviour of our samples, the parameters of the finite stack model have to be set with $\sigma_x > 0.25$ and $N \leqslant 2$. Taken literally, a stack of less than two lamellae is an arbsurdity. Even when viewed from the statistical point of view, the model presents conceptual difficulties. To be consistent with the experimental results, the model requires σ_x to increase and N to decrease as the crystallization cooling rate is slowed down. This implies an overall decrease in order at slower crystallization rates and is opposite to the normal expectations of a lamellar system. In principle it should be possible to use electron microscopy to distinguish stacks of two lamellar from the 'infinite' stacks of the other models.

According to the variable stack model, a lower crystallization rate implies an increase in stack dispersity σ_c but little change in lamellar dispersity σ_x. This trend could be explained by the effects of molecular segregation. When samples cool slowly, the less branched molecules will tend to crystallize first giving lamellar stacks of higher crystallinity and longer mean period. These will be progressively followed by lamellar stacks containing more highly branched species giving lower local crystallinities and smaller long periods. In contrast, fast quenching will prevent such large scale molecular segregation and will give lower interstack dispersity. Therefore, purely on the grounds of expected molecular behaviour, the basic principles of the variable stack model appear to be more appropriate. There however is no reason why features from both the variable stack and finite stack should not be present in the same sample.

In principle it should be possible to distinguish between these two model types from the asymptotic behaviour at zero angle. Using Gaussian statistics it can be shown from equation (4) that:

$$\frac{\lim_{s\to 0} I(s)}{\lim_{s\to\infty} [I(s)\cdot s^2]} = 2\pi^2\varphi^2(1-\phi)^2 \left(\frac{\sigma_y^2}{\bar{Y}^2} + \frac{\sigma_z^2}{\bar{Z}^2}\right) \bar{X}^2$$

This relationship will hold for all models with 'infinite' stacks, including the variable stack model. For all practical purposes it follows from this relationship that the asymptote is mainly governed by the lamellar dispersity σ_x. For the finite stack case, the intensity will start to follow the same tendency as for infinite stacks, but will then rapidly increase again as the central scatter from $I_c(s)$ becomes dominant. Although the experimental curves are limited by the incident beam backstop, estimates of the asymptotic trend indicate that for all samples σ_x is in the range 0.1 to 0.15. This is less than the estimates in *Table 5* based on a match with the variable stack model, but it is more easily accomodated by it than by the finite stack model. The extent of the disagreement may be a function of the specific variable stack model chosen. Other variable stack types may be better – e.g. if the lamellar dispersity σ_x as well as the long period of each stack varied with crystallinity.

It should be noted that it was the asymptotic behaviour that led Strobl and Muller[4] to conclude that LDPE must have a finite stack dispersity. They estimated that the fluctuation δL of the long period L between different stacks was $\delta L/L \simeq 0.8$. Translated to our specific variable stack model this degree of dispersion is equivalent to $\sigma_c \simeq 0.2$, i.e. close to the fitted values in *Figures 2* to *5*.

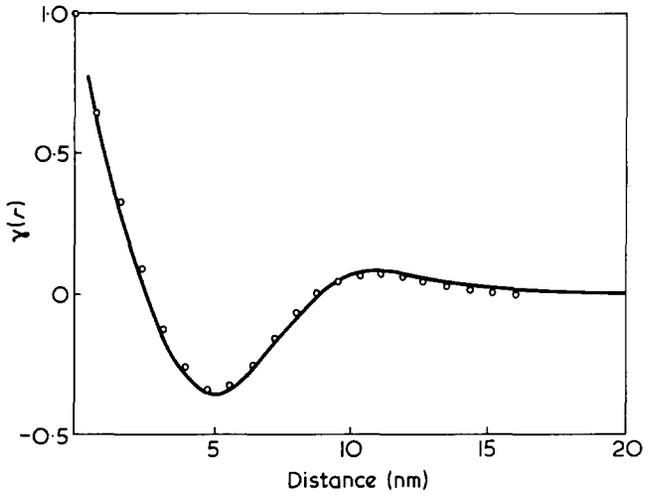

Figure 5 Correlation function for sample 5, with superimposed, scaled theoretical points for the variable stack model with $\phi = 0.5$, $\sigma_X = 0.2$, $\sigma_C = 0.25$

The presence of a variation in crystallinity between stacks can have consequences in the interpretation of other aspects of low-angle X-ray data. One important factor that would be affected is the overall scattering power as measured by the so-called 'invariant'. For the variable stack model the one-dimensional form of the invariant will be:

$$\int_{-\infty}^{\infty} I(s)\mathrm{d}s = (\rho_c - \rho_A)^2 \{\bar{\phi}(1-\bar{\phi}) - \sigma_c^2\}$$

The magnitude of the invariant will therefore decrease with increasing σ_c and will be most affected when ϕ is either very large or very small.

With regard to interpreting the long period, the presence of stack dispersity can have some beneficial consequences in interpreting the Bragg long period. Much attention with theoretical models has been given in the literature to the structural factors which can cause a distortion of the peak shape[2] and hence give a false impression of the average long period. The results in *Tables 1* to *4* serve as a summary of some of these effects. In all the model calculations, the number-average long period of the lamellar stacks have been defined to be unity. Thus the observed values of L_1 and L_2 in the *Tables* indicate the variations in distortion introduced by the various choices of model parameters and statistics. It will be noted that for $\phi = 0.5$ and $W_{1/2} \gtrsim 0.7$, that the degree of distortion in *Table 1* for the infinite stack model is high (~25%) whereas in *Table 4* for the variable stack model the distortion is lower (~10%).

This shows that the deduced Bragg long period will be closer to the true number-average when the peak broadening is due to stack dispersion than when it is solely due to lamellar dispersity.

CONCLUSION

The investigation has shown that it is more fruitful and less misleading to make comparisons using both $I(s)$ and $\gamma(r)$ curves rather than relying on just one of them. The comparisons have shown that the simple 'infinite' stack type of model is inappropriate for LDPE. The finite stack and variable stack type of models give much better fits to the experimental curves. Of these two, the implications and evidence favour the variable stack model as being more realistic. This however does not mean that the specific details employed in the model are all correct but rather that the principle of a dispersity of stacks coupled with the crystallinity fluctuation represent the type of characteristics of a one-dimensional model needed to describe the structure. These characteristics give a lower distortion to the position of the diffraction peak and thus give the satisfaction of implying that despite the very broad peak, the observed long period is closer to the true number-average period than would be implied by the simple infinite stack model.

ACKNOWLEDGEMENTS

I thank Dr C. G. Vonk for the donation of his FFSAXS Fortran Program, H. R. Pearson for writing the analysis routines and D. R. Beckett for preparation of samples.

REFERENCES

1 Rheinhold, C., Fischer, E. W. and Peterlin, A. *J. Appl. Phys.* 1964, **35**, 71
2 Crist, B., *J. Polym. Sci. (Polym. Phys. Edn)* 1973, **11**, 635
3 Kilian, H. G. and Wenig, W. *J. Macromol. Sci. (B)* 1974, **9**, 463
4 Strobl, G. R. and Muller, N. *J. Polym. Sci.* 1973, **11**, 1219
5 Brown, D. S., Fulcher, K. U. and Wetton, R. E. *Polymer* 1973, **14**, 379
6 Tsvankin, D. Y. *Polym. Sci. USSR* 1964, **6**, 2358
7 Bramer, R. *Colloid Polym. Sci.* 1974, **252**, 504
8 Vonk, C. G. and Kortleve, G. *Kolloid Z. Z. Polym.* 1967, **220**, 19
9 Kortleve G. and Vonk, C. G. *Kolloid Z. Z. Polym.* 1968, **225**, 124
10 Ruland, W. *Colloid Polym. Sci.* 1977, **255**, 417
11 Hosemann, R. and Bagchi, S. N. 'Direct Analysis of Diffraction by Matter' North Holland, Amsterdam, 1962
12 Blundell, D. J. *Acta Crystallogr. (A)* 1970, **26**, 472; **26**, 476
13 Vonk, C. G. *J. Appl. Crystallogr.* 1973, **6**, 81
14 Ruland, W. *J. Appl. Crystallogr.* 1971, **4**, 70